Electronic Supplementary Material (ESI) for RSC Advances.

Towards an improved understanding of liquid transportation along a hair fiber: ratchet-like microstructure induced capillary rise

Xianliang Sheng[†,*], *Hongming Bai*[‡], *Jihua Zhang*[§,*]

[†] College of Science, Inner Mongolia Agricultural University, Hohhot, 010018, P. R. China.

[§]Aerospace Research Institute of Material and Processing Technology, Beijing, 100076, P. R. China.

[‡]Meinders School of Business, Oklahoma City University, 73106-1493, USA.

[*]X. Sheng (shengxl@iccas.ac.cn) and J. Zhang (zjhicca@iccas.ac.cn) are equal corresponding authors.

A simple discussion about the calculation of static meniscus profile when the conical frusta contact the hexane.

A conical frustum with rise angle ω is lowed to contact liquid surface vertically. When a liquid is contacted, it climbs along the solid surface and a meniscus is forced to develop. An illustration of liquid meniscus is presented in Figure S1a.

The curve profile of meniscus leads to the Laplace pressure difference ΔP given by Laplace equation:

$$\Delta P = P_1 - P_2 = \gamma\left(\frac{1}{R_1} + \frac{1}{R_2}\right) \quad \text{(S1)}$$

where R_1 is the radius of a circle of contact to the interfacial surface, which is in a plane perpendicular to the paper; R_2 is the radius of a circle of contact which is in the plane of the paper, γ is the interfacial tension.

For the planar wall with the infinite curvature of R_1, the balance of hydrostatic pressure with the Laplace pressure[S1, S2]:

$$\frac{1}{R_2} = -\frac{d\cos\psi}{dz} = \frac{\Delta\rho g z}{\gamma} \qquad \text{(S2)}$$

gives a solution of static meniscus shape ($\psi(x=0)=0$ and $dz/dx(x=0)=0$):

$$\bar{x} = \left[In\left\{ \frac{1+\cos(\psi/2)}{\sin(\psi/2)} \right\} - 2\cos\frac{\psi}{2} \right] + C \qquad \text{(S3)}$$

$$\bar{z} = 2\sin\frac{\psi}{2} \qquad \text{(S4)}$$

where the coordinate x and z are taken to be the horizontal and vertical directions (see Figure S1a), respectively; h is the location of intersection of liquid surface with the plate; ψ is the inclination angle of meniscus; The quantities with an overbar (-) indicate the length nondimensionalized by the capillary constant a; C is the integral constant. Equilibrium z_e of the meniscus can be given:

$$\bar{z}_e = 2\cos\frac{\omega+\theta_e}{2} \qquad \text{(S5)},$$

and corresponding $$\bar{h}_e = 2\cos\frac{\omega+\theta_e}{2} / \sin\omega . \qquad \text{(S6)}$$

where θ_e is equilibrium contact angle of liquid on the solid surface.

Figure S1b shows the catenary's shape of the meniscus calculated by eq S3 and S4, which expresses that the shape is the same when the liquid is at the right or at the left of the solid wall.

Dynamically, if assuming that pressure quickly equilibrates as the rise occurs, $v=dh/dt$ can be expressed as eq. 6: $v = -\left[\sin\frac{\omega+\theta(t)}{2} / \sin\omega \right] \frac{d\theta}{dt}$.

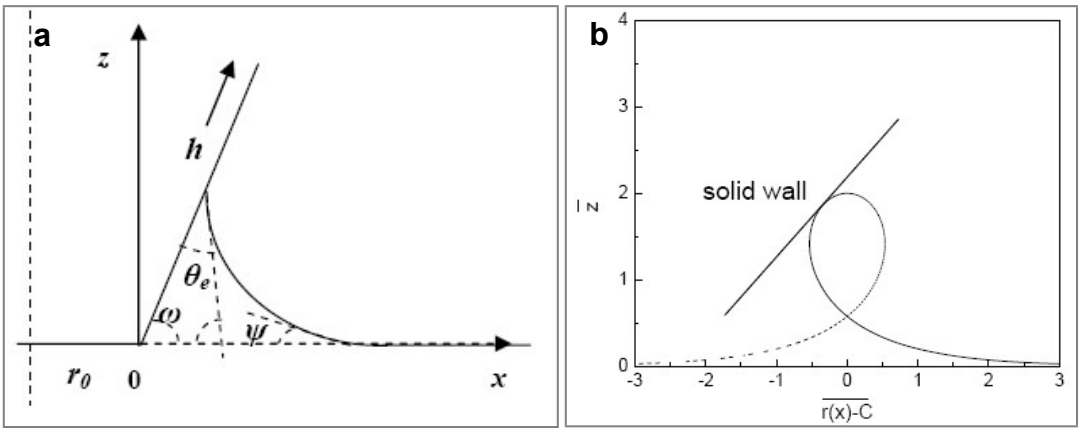

Figure S1 a) Schematic illustration of the capillary rise around conical frustum, where the rise angle is ω, ϕ is the inclination angle of meniscus, r_0 is the bottom radius of conical frustum, h is the climb length along the side surface of conical frustum. b) The static meniscus shape calculated by eq S3 and S4.

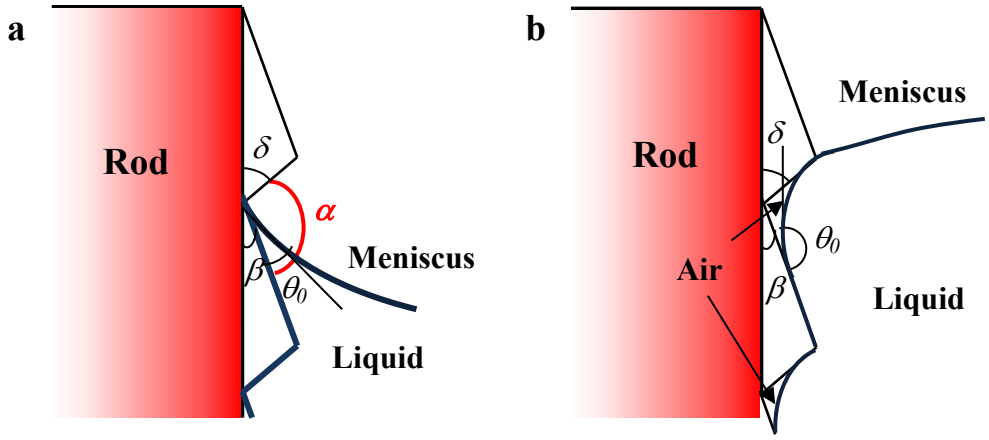

Figure S2 Different states of liquid contacting rough ratchet-like sides. Blue line indicates the contact line of meniscus. (a) Complete wetting; (b) composite interfaces on the ratchet-like structures

Here, a rod is selected as the typical example of conical frustum. Obviously, due to the angles of δ and β from ratchet-like structures, the angle α (*i. e.* $\pi - \delta - \beta$) forms on the microstructures of rod. When the contact angle θ_0 of meniscus is beyond α, liquid cannot completely invade the ratchet-like microstructures. So there are composite interfaces on the rough sides that composed by air, liquid and solid surface of rod (see Figure S2). The apparent contact angle can be expressed by Cassie equation (eq. 3). But on the condition of $\theta_0 \leq \alpha$, liquid completely invade the ratchet-like microstructures, *i.e.* at Wenzel state.

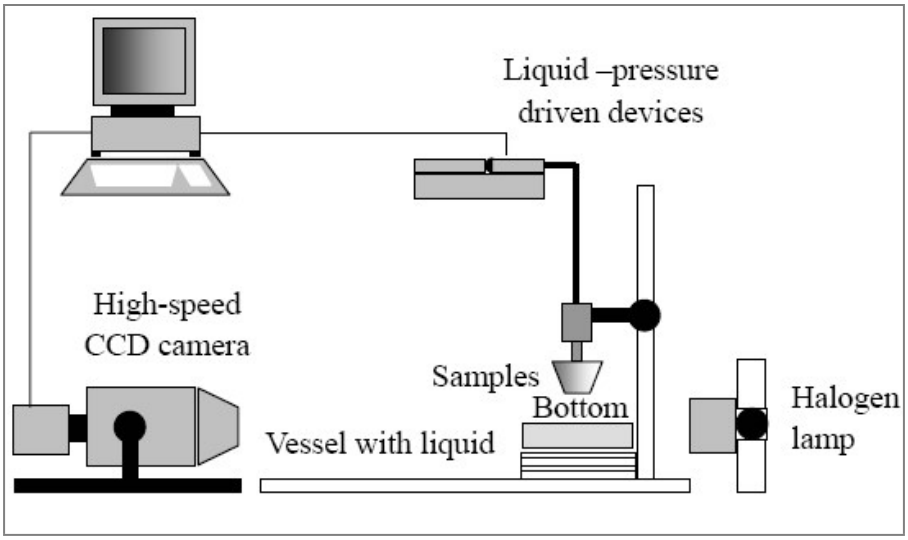

Figure S3 Schematic diagram of the experimental setup.

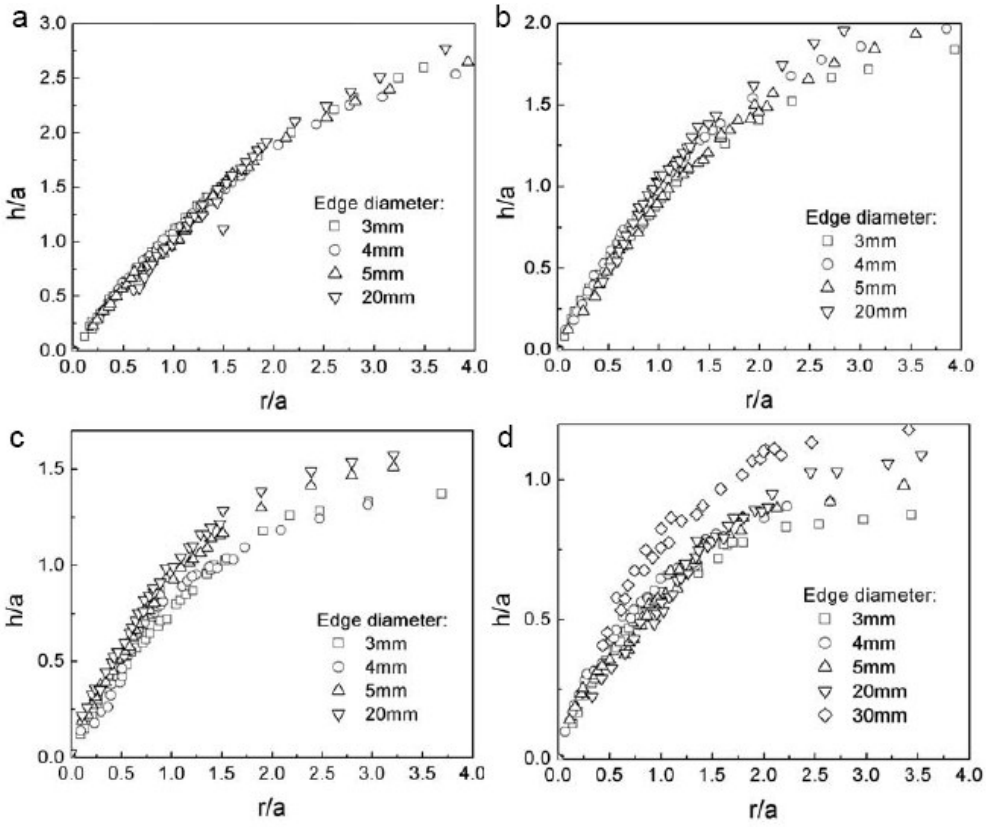

Figure S4 The (h/a) versus (r_x/a) plots of the Al conical frusta with various sizes during the capillary rise, where a is the capillary constant, for water, a = 2.7 mm: (a) ω = 30°, (b) 45°, (c) 60° and (d) 90°, respectively. The linear relations are found at the early stage of all curves (ω=30°, 45°, 60° and 90°). The meniscus shape can be approximated by the simple linear relation of $r = (k+\cos\omega)h$ where k is a constant.

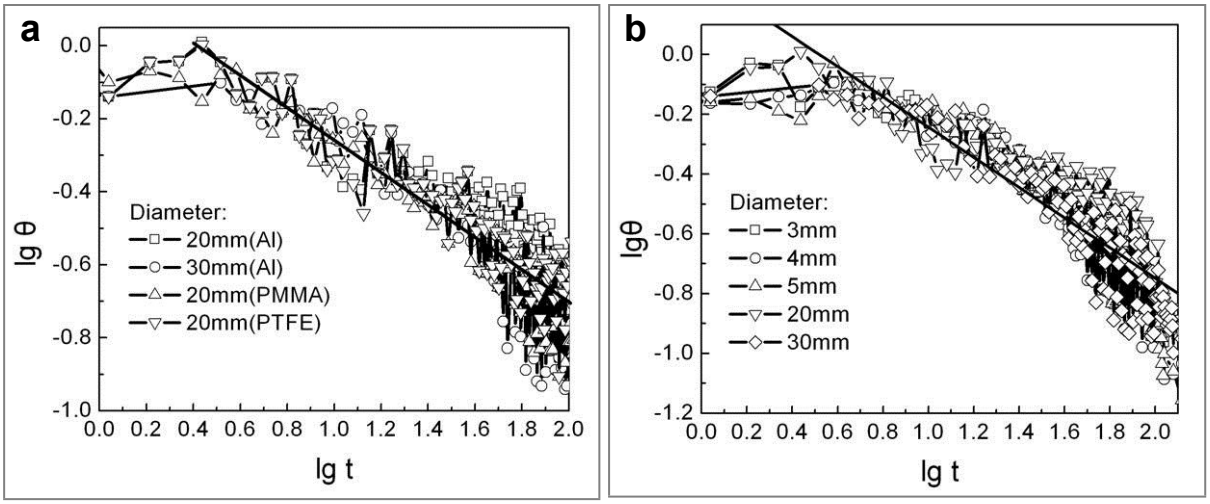

Figure S5 The plots of $\lg\theta$ - $\lg t$ for solid rods corresponding to Figure 6: a) solid rods with different surface tensions; b) Al rods with d_0 = 3, 4, 5, 20 and 30 mm.

Further discussion about the equilibrium and steady contact angle along the hair fiber during the meniscus rise.

The equilibrium contact angle can be theoretically defined by the famous Young equation. The surfaces considered in the Young equation are perfectly smooth and homogeneous and the state of the system is an equilibrium state. In our experimental situation, the hair fibers do not have smooth and homogeneous surfaces or to be in a true equilibrium state. Indeed, our meniscus profile is not fully equivalent to the "equilibrium" meniscus. Its contact angle should lie somewhere between those of the advancing and receding contact angles[S3]. A theoretical approach to calculate the equilibrium angle was published by Tadmor [S4]. If advancing and receding contact angles result from the surface roughness and heterogeneity being distributed in an isotropic way on the surface, the resistance of the three-phase solid/liquid/air line to the motion out (advancing mode) will equal the resistance of the motion in (receding mode). Then an equation relating the advancing θ_A, receding θ_R, and equilibrium θ_e contact angles is derived,

$$\theta_e = \arccos\left(\frac{\Gamma_A \cos\theta_A + \Gamma_R \cos\theta_R}{\Gamma_A + \Gamma_R}\right) \qquad \text{S1}$$

where

$$\Gamma_R = \left(\frac{\sin^3\theta_R}{\left(2 - 3\cos\theta_R + \cos^3\theta_R\right)}\right)^{1/3}$$

and

$$\Gamma_A = \left(\frac{\sin^3 \theta_A}{\left(2 - 3\cos\theta_A + \cos^3 \theta_A\right)} \right)^{1/3} .$$

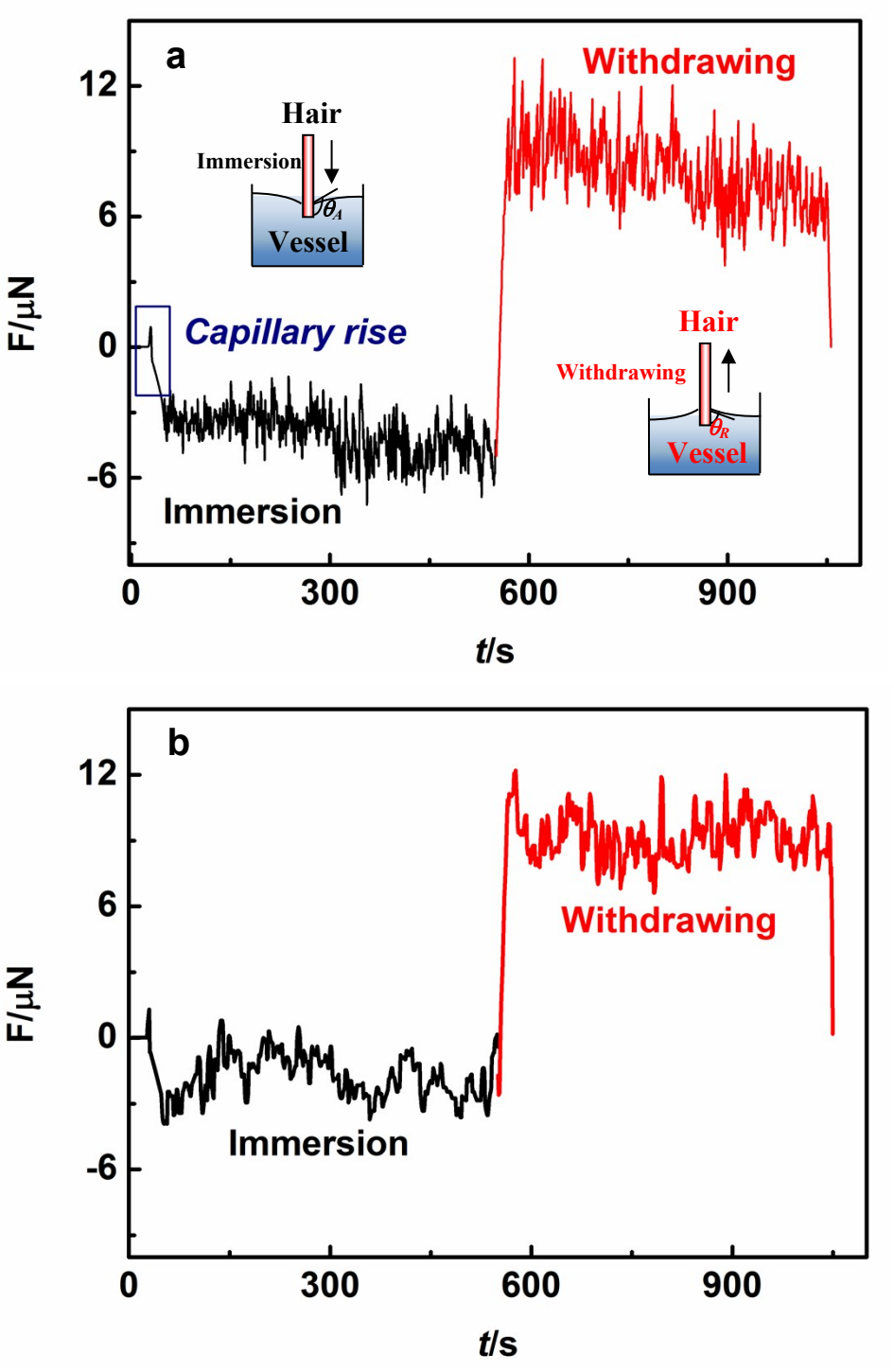

Figure S6 The typical plots of force versus time for different parts of hair during hair fiber contacts, immerses and then is withdrawn from the water: (a) at the middle and lower part of the single hair; (b) at its middle part.

We complete the plots of capillary force versus time when hair fiber is immersed into water and then withdrawn at the velocity of 0.01 mm/s (see Figure S6a and b). The average values of θ_A and θ_R are calculated as ~98° and ~67° by the plots, respectively. The equilibrium contact angle is obtained by using eq. S1. It is theoretically obtained as 77°. In contrast with the observation in Fig. 8, the calculated contact angle is lower than the experimental one (~84°). So it is stressed that the measured contact angle by the static meniscus is only a steady one, not necessarily the equilibrium one. It is impossible to develop a meniscus at "zero" speed, so the measured contact angle on the hair is higher or lower than the equilibrium one. Similarly, it is true for the meniscus height.

Based on the above discussions, the wetting of hair fiber is complicated by pinning of the contact line. Pinning prevents the meniscus from reaching its equilibrium profile. We further calculate the pinning force of $F_{pinning}$ as ~8.5 μN by the difference between θ_A and θ_R: $F_{pinning} = 2\pi r_0 \gamma \left(\cos\theta_R - \cos\theta_A\right)$, where r_0 is the average radius of the hair fiber, and γ is surface tension of liquid. The value is far more than the capillary force (~1.42 μN).

In addition, it should be noticed that the aspects at different parts of hair fiber are not completely same. There are slightly different sizes (transitional sizes), microstructures and defects for them [S5]. In the experiments, we choose the middle parts of the hair (the length of ~8 mm) as the samples. Due to water absorption, hair fiber sample is only employed for one time in the experiment. But it still slightly different for the similar parts of the same hair (see the force curves in Fig. S6a and b). So we obtain the average immersion (advancing) forces or withdrawing (receding) ones for each round of experiments and then average them (three samples) as the final results. We calculate the advancing or receding angles by these average values.

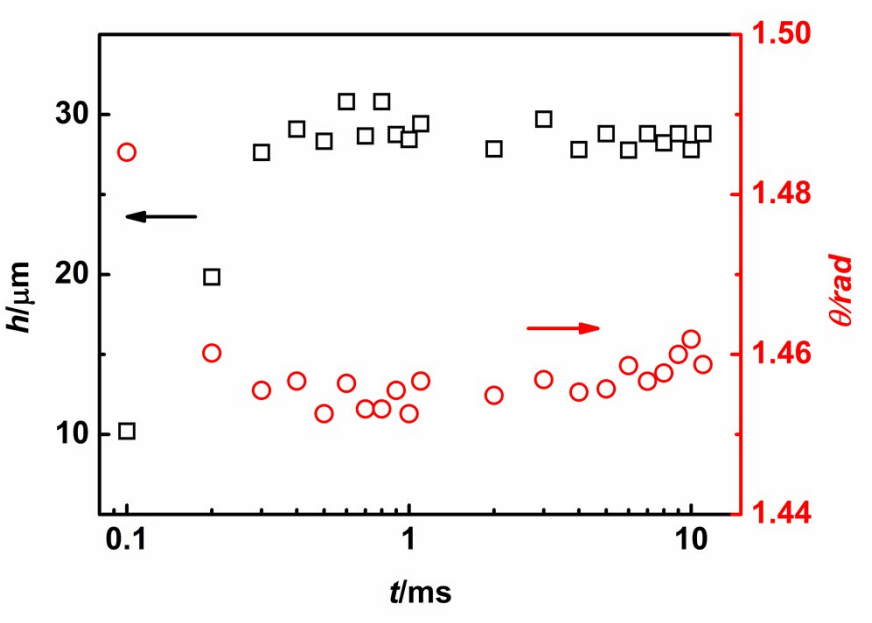

Figure S7 The plots of wetting height (h, the square symbol of □) and contact angle (θ, the hollow circular symbol of ○) versus contacted time (t) for the hair fiber during the capillary rise of water. Obviously, there is few data to show the whole process.

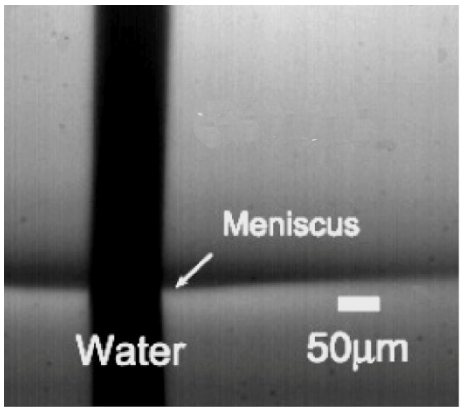

Figure S8 Optical images of an unclean hair fiber contacting the water. Even if water surface is deformed a little, capillary rise cannot occur.

Video S1 Oscillations of the whole meniscus wetting along the surface of Al sample with d_0 =3 mm and ω=60°.

Video S2 Dynamic meniscus of hexane along the clean hair fiber.

Video S3 Dynamic meniscus of water along the clean hair fiber.

Reference

[S1] J. D. Eick, R. J. Good, A. W. Neumann, *J. Colloid Interface Sci.*, **1975**, 53, 235.

[S2] S. Hartland, in Surface and Interfacial Tension, Marcel Dekker, Inc., New York, 2004, Chapter 7.

[S3] E. Pierce, F.J. Carmona, A. Amirfazli, *Colloid Surf. A*, **2008**, 323, 73.

[S4] R. Tadmor, *Langmuir*, **2004**, 20, 7659.

[S5] R. A. Lodge, B. Bhushan, *J. Appl. Polym. Sci.*, **2006**, 102, 5255.